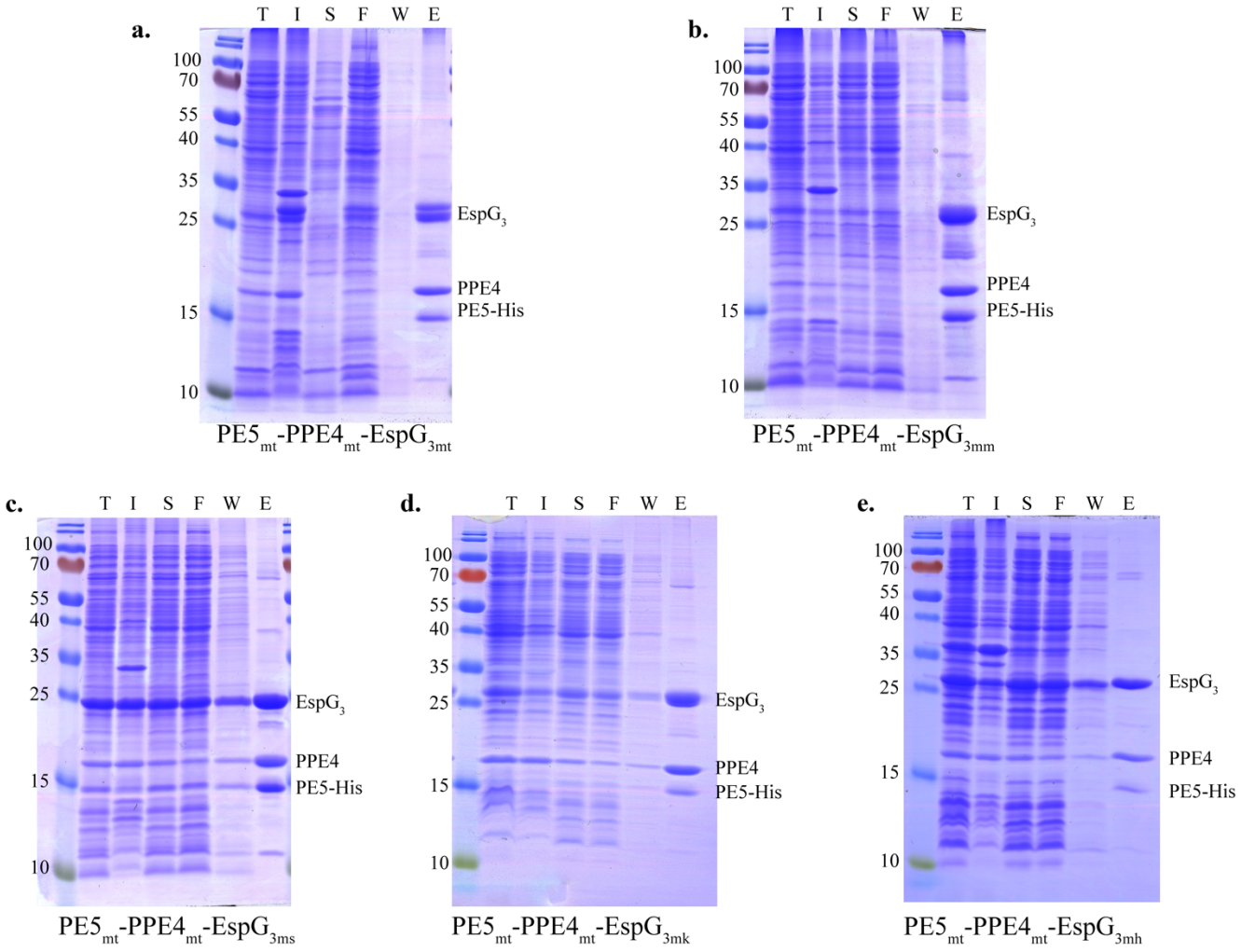

Supplementary Figure 1. $PE5_{mt}$-$PPE4_{mt}$ dimer is bound by $EspG_3$ from various mycobacterial species. Co-purification of $PE5_{mt}$-$PPE4_{mtb}$with *a,* $EspG_{3mt}$, *b,* $EspG_{3mm}$, *c,* $EspG_{3ms}$, *d,* $EspG_{3mk}$, or *e,* $EspG_{3mh}$. T is total lysate, I is insoluble lysate, S is soluble lysate, F is column flow through, W is column wash, and E is column elution.

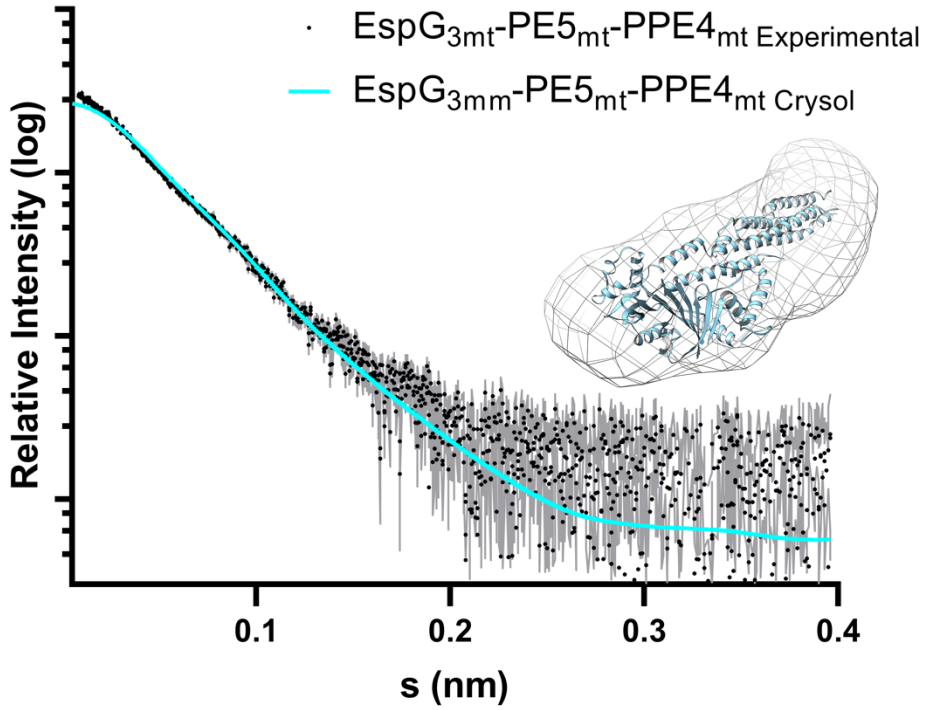

Supplementary Figure 2. Comparison of $PE5_{mt}$-$PPE4_{mt}$-$EspG_{3mm}$ crystal structure and $PE5_{ms}$-$PPE4_{ms}$-$EspG_{3ms}$ SAXS data. The SAXS data was originally collected in (ref) and compared to the 6UUJ structure we obtained. The χ^2 between the crystal structure and SAXS data is 2.53 as compared by CRYSOL (ref). An insert shows the 6UUJ structure inside an envelope created by GABSOR (ref).

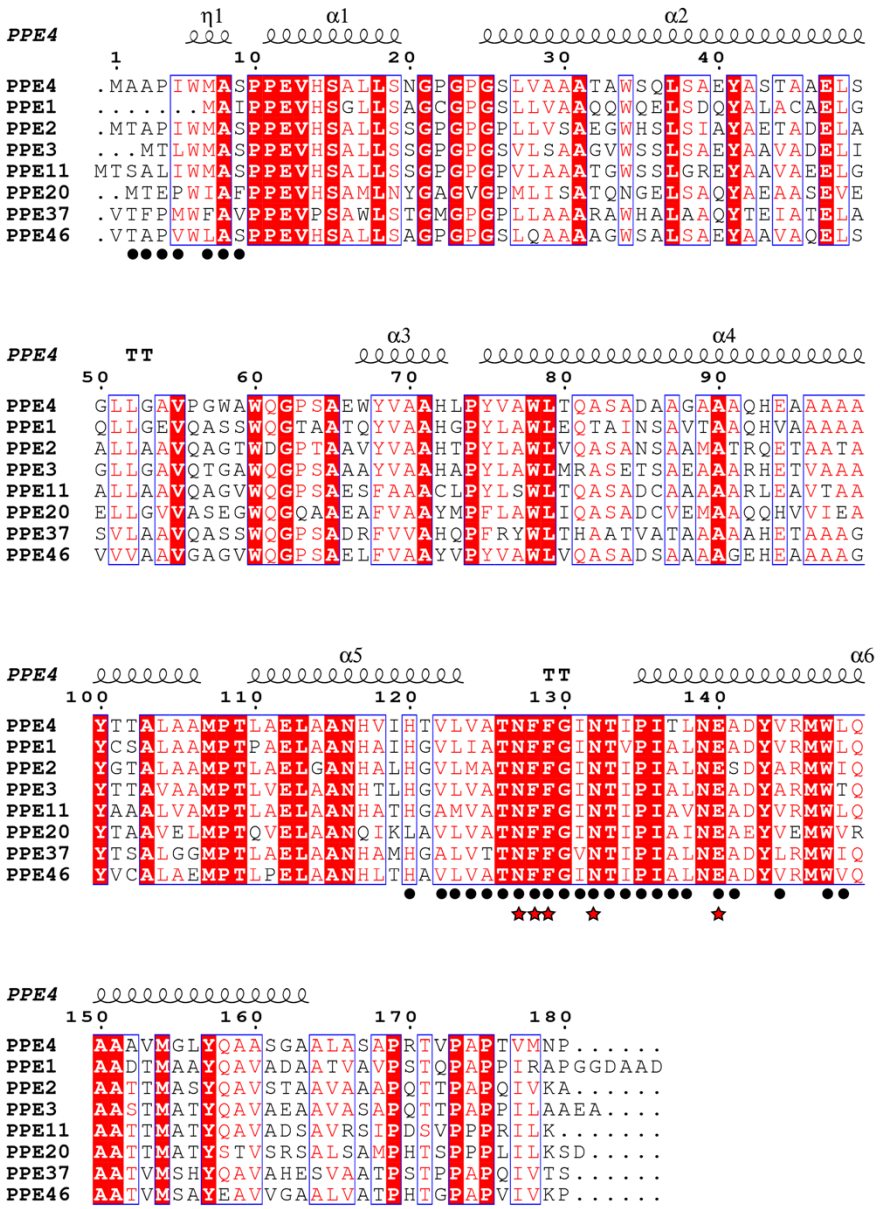

Supplementary Figure 3. Sequence alignment of *M. tuberculosis* ESX-3-specific PPE genes. Genomic sequences of *M. tuberculosis* PPE proteins were aligned with Clustal. The secondary structure from $PPE4_{mt}$ from the trimer model (6UUJ) is shown above each row of the alignment. Residues that are identical across all of the ESX-3-specific PPEs are highlighted in red. Residues interacting with $EspG_{3mm}$ in the crystal structure are denoted with black circles and the ones that were chosen for mutagenesis are denoted with a red star.

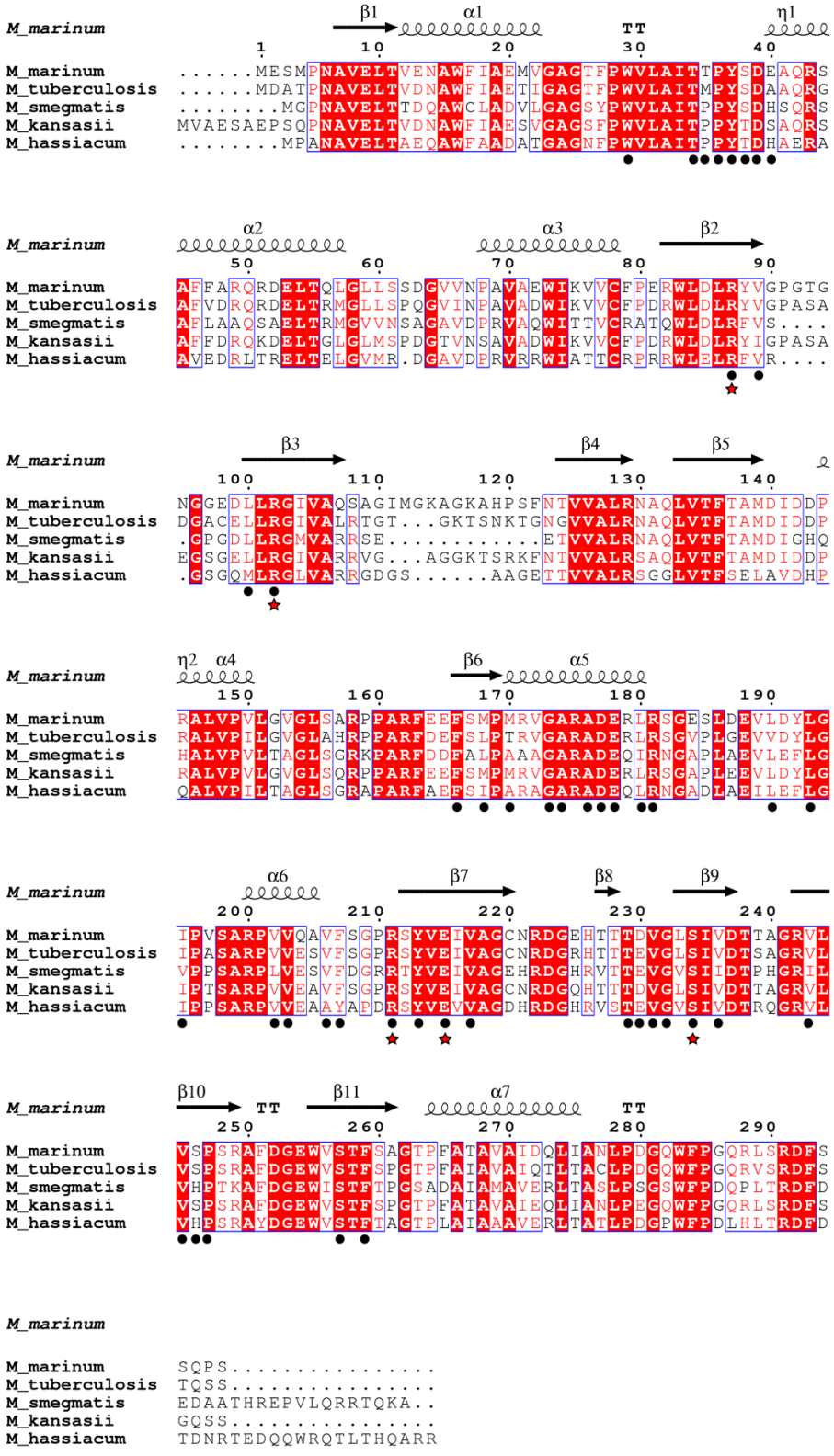

Supplementary Figure 4. Sequence alignment of selected EspG$_3$'s shows interacting residues are conserved. Genomic sequences of the five EspG$_3$s used in this study were aligned using Clustal. The secondary structure from EspG$_{3mm}$ from our trimer model (6UUJ) is shown above each row of the alignment. Residues that are identical across the five species are highlighted in red. Residues interacting with PPE4$_{mt}$ in the crystal structure are denoted with black circles and the ones that were chosen for mutagenesis are denoted with a red star.

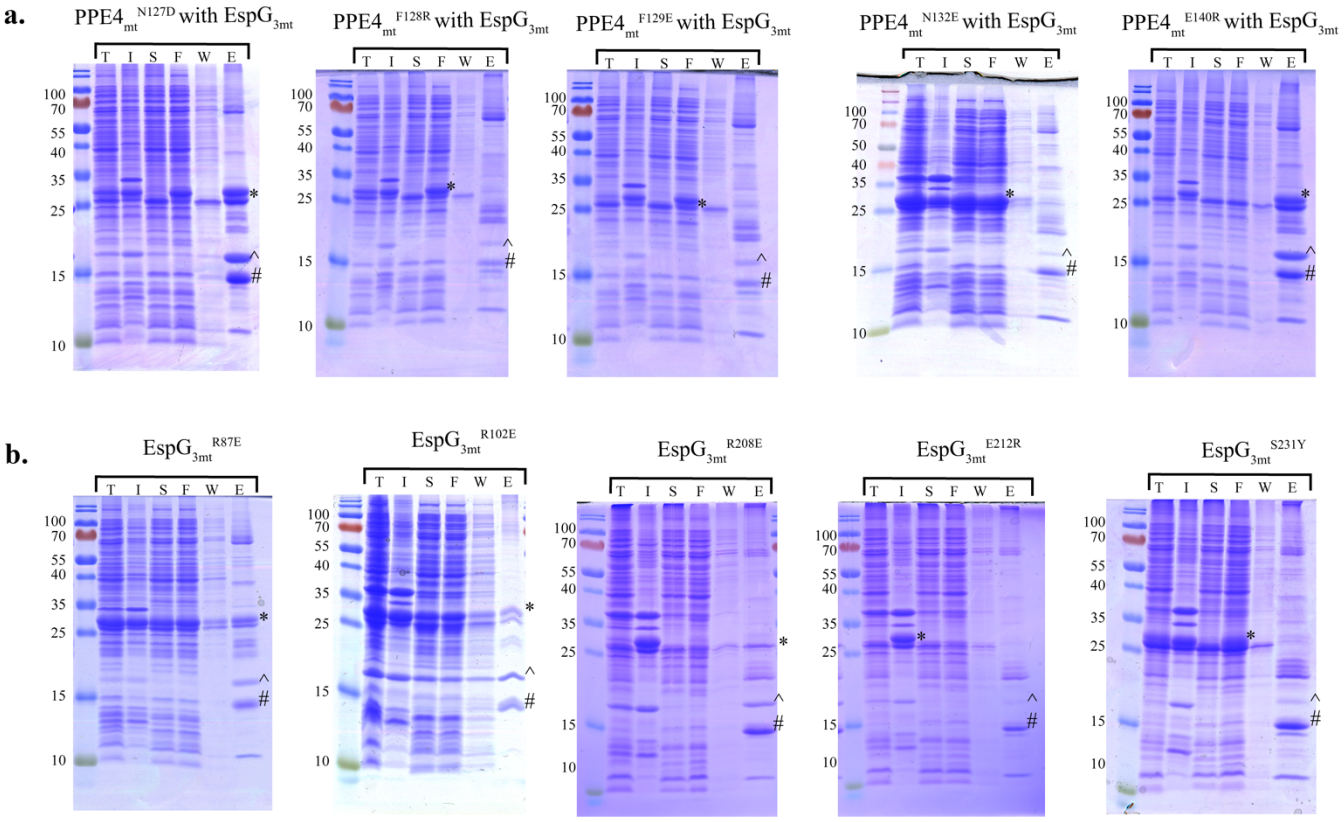

Supplementary Figure 5. Co-purification of selected $PPE4_{mt}$ and $EspG_{3mt}$ mutants with their wild-type partners. Gels from co-purification pulldowns of $PPE4_{mt}$ (*a*) and $EspG_{3mt}$ (*b*) mutations show which mutations disrupt the $PPE4_{mt}$-$EspG_{3mt}$ interface ($PPE4_{mt}^{F128R}$, $PPE4_{mt}^{F129E}$, $EspG_{3mt}^{E212R}$, $EspG_{3mt}^{S231Y}$), and which do not. Results are summarized in Table 2. Each protein is denoted with a unique symbol in each gel; $PE5_{mt}$ (^), $PPE4_{mt}$ (#), and $EspG_{5mt}$ (*). T is total lysate, I is insoluble lysate, S is soluble lysate, F is column flow through, W is column wash, and E is column elution. The identity of $PE5_{mt}$, $PPE4_{mt}$, and $EspG_{5mt}$ was confirmed by mass-spectrometry analysis.

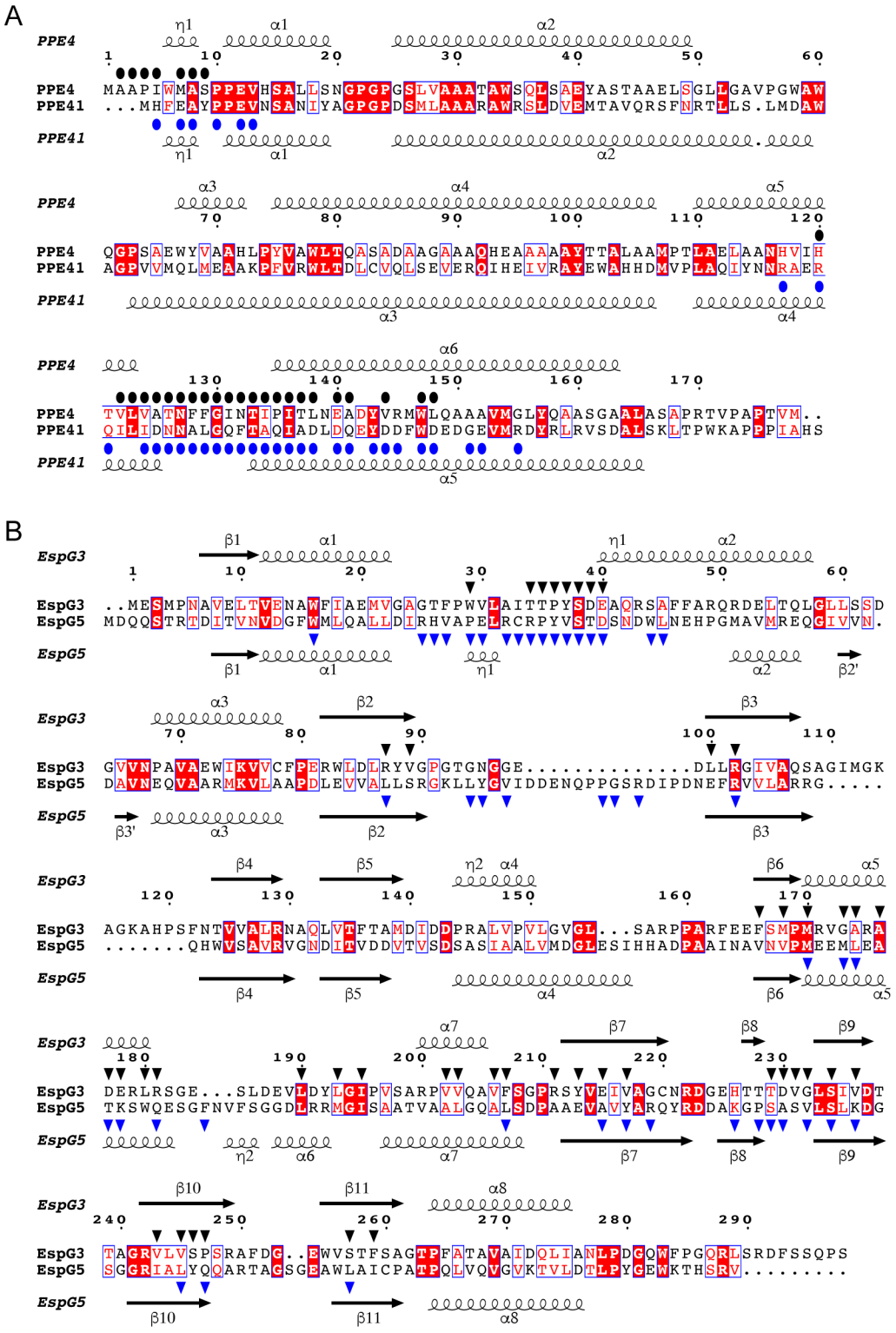

Supplementary Figure 6. Comparison of interfaces in the ESX-3- and ESX-5-specific PPE-EspG complexes. *A*, Structure-based sequence alignment of PPE4 (6UUJ) and PPE41 (4KXR). Residues interacting with $EspG_{3mm}$ and $EspG_{5mt}$ chaperones are indicated with black and blue circles, respectively. *B*, Structure-based sequence alignment of $EspG_{3mm}$ and $EspG_{5mt}$. Residues interacting with PPE4 and PPE41 are indicated with black and blue triangles, respectively.

Supplementary Table 1. Summary of constructs utilized for crystallization experiments and final outcomes.

PE5 construct (all constructs contain His_6 purification tag)	**PPE4 construct (only N-terminal PPE domain)**	**$EspG_3$ construct**	**Crystallization Outcome**
MSMEG_0618	*MSMEG_0619*	*MSMEG_0622*	Low resolution crystals
MSMEG_0618 with MBP fusion (two different linker lengths)	*MSMEG_0619*	*MSMEG_0622*	Low resolution crystals for both linker lengths
MSMEG_0618 with T4L fusion (3 different forms of T4L)	*MSMEG_0619*	*MSMEG_0622*	Poor expression of trimer in all forms
Rv0285	*Rv0286*	*Rv0289*	Low resolution crystals
Rv0285	*Rv0286*	*MMAR_0548*	Two crystal forms solved